DRONE NET, A PASSIVE INSTRUMENT NETWORK DRIVEN BY MACHINE VISION AND MACHINE LEARNING TO AUTOMATE UAS TRAFFIC MANAGEMENT

Sam Siewert[*], Mehran Andalibi[†], Stephen Bruder[‡], Iacopo Gentilini[§], Aasheesh Dandupally, Soumyatha Gavvala, Omkar Prabhu,[**] Jonathan Buchholz[††] and Dakota Burklund[‡‡]

Herein we present an overview of an experimental design to validate and verify key aspects of the Drone Net system architecture, a design to provide detection, tracking, and classification/identification of aerial systems, both piloted and unmanned. We have a cost competitive solution based on EO/IR (electro-optical and infrared) passive sensing combined with acoustics and networking of these elements such that we can use machine vision and machine learning to be able to catalog all aerial objects within a volume. The experiment we have constructed and tested with preliminary UAS traffic management scenarios (urban and rural) will allow us to assess the feasibility of using passive sensing compared to higher cost RADAR and to determine if we can match, or perhaps even outperform RADAR in terms of classification and identification. Finally, we present concepts for an order of magnitude lower cost system design which can be integrated with UAS traffic management and interfaced with ATC (Air Traffic Control) compared to active sensing. To test integration with ATC, we are working with our aviation program at Embry Riddle. Preliminary results presented here indicate promise for our EO/IR + acoustic-based UTM.

INTRODUCTION

Drone Net is an architecture to integrate passive and active sensor nodes in a network for small Unmanned Aerial Systems (sUAS) traffic management. The goal of the proposed research

[*] Assistant Professor, Computer, Electrical, and Software Engineering, Embry Riddle Aeronautical University, 3700 Willow Creek Rd, Prescott, AZ 86301.
[†] Assistant Professor, Mechanical Engineering, Embry Riddle Aeronautical University, 3700 Willow Creek Rd, Prescott, AZ 86301.
[‡] Associate Professor, Computer, Electrical, and Software Engineering, Embry Riddle Aeronautical University, 3700 Willow Creek Rd, Prescott, AZ 86301.
[§] Associate Professor, Mechanical Engineering, Embry Riddle Aeronautical University, 3700 Willow Creek Rd, Prescott, AZ 86301.
[**] Embedded Systems Engineering Master's students, Electrical, Computer and Energy Engineering, CU Boulder, 80309-0425.
[††] Undergraduate student, Mechanical Engineering Robotics, Embry Riddle Aeronautical University, 3700 Willow Creek Rd, Prescott, AZ 86301.
[‡‡] Undergraduate student, Aerospace Engineering, Embry Riddle Aeronautical University, 3700 Willow Creek Rd, Prescott, AZ 86301.

architecture is to evaluate the use of multiple passive sensor nodes with Electro-Optical/Infrared (EO/IR) and acoustic arrays networked within a UAS Traffic Management (UTM) operating region such as "class G" uncontrolled airspace. The Drone Net approach will be compared to and/or used in addition to RADAR (Radio Detection and Ranging) and Automatic Dependent Surveillance-Broadcast (ADS-B) tracking and identification. While ADS-B, with 50 kHz bandwidth at 1090 MHz, is a viable solution for general aviation tracking, the sample and broadcast rates for position and identification have limited precision and frequency. ADS-B alone may not be sufficient for UAS tracking in much smaller class G airspace operating regions with many UAS.

We hypothesize that a network of passive sensors will be a more cost effective approach to manage small UAS that are both compliant and non-compliant (sUAS without ADS-B transceivers) compared to RADAR and ADS-B alone. While the primary goal of Drone Net is security and safety for sUAS operations in urban and rural regional operating regions at 400 AGL (Above Ground Level), the project is also working with Embry Riddle's ATC program to explore integration of automated UTM into ATC grid management of class G National Air Space (NAS) in general. The vision is full automation of UTM at the grid level with ATC contingencies managed by Automated Flight Service Stations (AFSS).

The network of Drone Net instruments in a local area as well as regional and more global cloud-based networks will allow for heterogeneous information fusion and algorithm development for multi-sensor drone detection, classification, and identification with more accuracy than a of a single database. The power of the Drone Net project is the open design as well as data sharing to improve data mining and machine learning over time. Applications for Drone Net include UTM, but also safety and security for campus and public venues in general. Large shared data sets combined with cloud-based machine learning and aggregation of detection methods within a growing network is expected to outperform point solutions.

The project includes definition of machine learning metrics to compare commercial and research systems designed for UTM with automated generation of Precision and Recall (PR), harmonic mean of PR, or F-measure, and Receiver Operator Characteristic (ROC) analysis as well as methods of human review. Ultimately the intent is to integrate with ATC for contingency management by assisting with grid-based management of drones in a class G column of air, cataloging all expected aerial objects and noting any that are unexpected and/or non-compliant. Normal operations in UTM are envisioned to require simple coordination via UAS flight plan filings and ATC notices to aircraft (NOTAMs).

In the remainder of this paper, we present current test data from Embry Riddle and discuss collaboration efforts with our ATC program and passive instrument network design in progress with University of Colorado Boulder to complete the open specification for ground and flight instruments including: all-sky camera, EO/IR narrow field, acoustic and flight Light Imaging, Detection, And Ranging (LIDAR) with Long Wave Infrared (LWIR). We would also like to invite others to participate to grow the network and the data available for research.

DRONE NET EXPERIMENT OBJECTIVES

The Drone Net system architecture [22] is intended to be a research test-bed for UAS traffic management experiments for both urban and rural settings, consistent with NASA UTM concepts for operations of drones in shared class-G airspace with general aviation. While there are available industry systems and products for drone detection, shields, counter UAS, and creation geofencing for airports [27, 28, 29, 30], our team wanted to create a fully open design with the goal to support machine vision, machine learning and detection, tracking, classification and identification performance metrics that are published. The software embedded in each EO/IR camera sys-

tem includes real-time MV/ML detection and classification for drone or not-drone (MV/ML) which has been shown to be feasible using a CNN (Convolutional Neural Net). Furthermore, part of our hypothesis for this experimental design is that Drone Net can be configured to provide competitive aerial object tracking and catalogs at an order of magnitude lower cost, with simplified deployment and operation (mostly autonomous) and simple integration with NASA UTM operational concepts as well as ATC (Air Traffic Control). In this paper, we report upon our experimental design, based on the architecture for Drone Net, and our first set of both rural and urban experiments. From this experience, we have also outlined goals and objectives for future experiments and how they align with UTM and ATC in general.

Experiment Feasibility

Our rural tests largely showed, as has also been determined by other NASA UTM partner program researchers, that rural operation is not without challenges, but less complicated than urban operation. Based on these preliminary comparative results, we have chosen to focus on urban testing, with emphasis on scenarios of interest to industry such as parcel delivery, remote inspection, surveys, and security use. In particular, our objective is to show that EO/IR + acoustic networks of sensors (Drone Net) combined with both compliant small UAS (cooperative Drone Net aerial node) and non-compliant can be effective tracked and classified and/or identified for a log of daily traffic, both on flight-plan and off, which is competitive with RADAR and other active sensing methods (LIDAR). Likewise, we assume that compliant sUAS will have ADS-B, but our Drone Net compliant sUAS will have LIDAR and EO/IR in addition for urban navigation. The first technical objective we have is therefore to compare the range of detection using EO/IR with RADAR. For this, we use simple optical equations for optical gain:

$$G = B \times \frac{(g - f')}{f'}, AR = \frac{H_{pixels}}{V_{pixels}}, H_{pixels} = \frac{D_{H_{section}}}{G} \times R_{H_{fov}}, V_{pixels} = \frac{D_{V_{section}}}{G} \times \mathrm{R}_{V_{fov}} \quad (1)$$

In Equation set (1), AR is aspect ratio, B is the object image size on the detector, f' is the focal length, g is the working distance, and G is the physical extent of an observable object. So, for example, the ALTA6 sUAS that we have tested with, which has a 1126 mm diameter, at a working distance of 617.5 meters using an LWIR (Long Wave Infrared) FLIR Boson detector with 6.0 degree H_{fov}, G=64.96 meters, so horizontal pixel extents in an image (H_{pixels}) for a 640 line-scan resolution of R_{Hfov}would be 11 pixels. Figure 1, shows a test image using a visible camera with a 55mm focal length for a 24mm detector, such that G=269.43 meters, and therefore 25 pixels for $H_{section}$ of 1126mm.

Figure 1. Visual Feasibility Test for Detection and Tracking at Working Distance

The key metric associated with EO/IR detection is that the object must be more than single pixel and ideally should appear as a pixel neighborhood that is at minimum 3x3, and preferably 8x8 for typical aspect ratios. For both cameras, we meet the minimum pixel neighborhood criteria given the lens pairings we have made for or experimental working distance.

Experiment Configuration

Given the feasibility testing and analysis to show that we can detect sUAS of interest, down to 1-meter $H_{section}$, we have created a coverage grid with our EO/IR instruments and all-sky detection cameras used in the Drone Net architecture as shown in Figure 2. The all-sky camera in the center provides 180 by 360 degree hemispherical coverage (at 6 x 2 megapixels or higher) to trigger narrow field EO/IR tracking with an initial azimuth and elevation triggered by simple motion detection. The EO/IR sensor will track based upon classification as a drone determined by MV/ML.

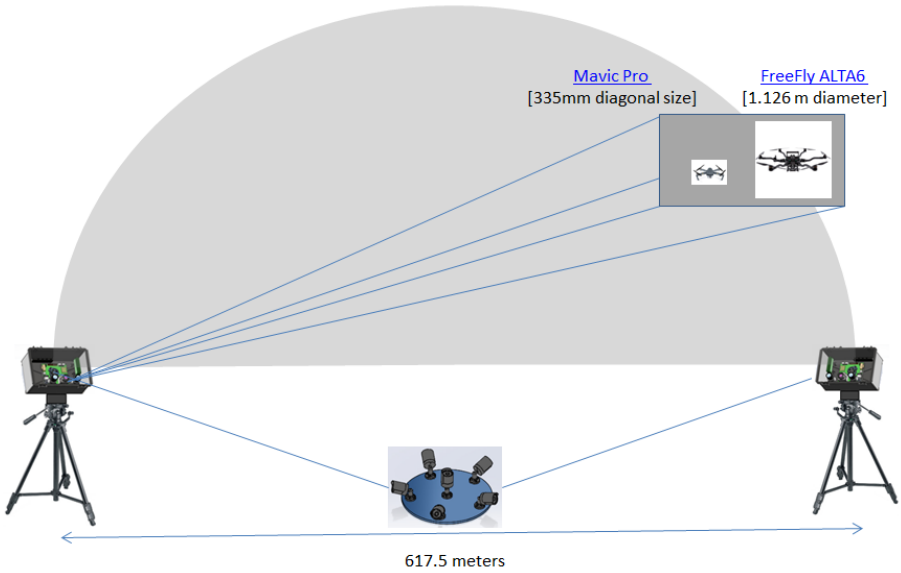

Figure 2. EO/IR and All-sky Camera Sensor Network for Drone Net Experiments

This basic working distance of 617.5 meters is based upon dimensions of the Embry Riddle Prescott campus with both urban regions of interest and semi-rural regions as shown in Figure 3.

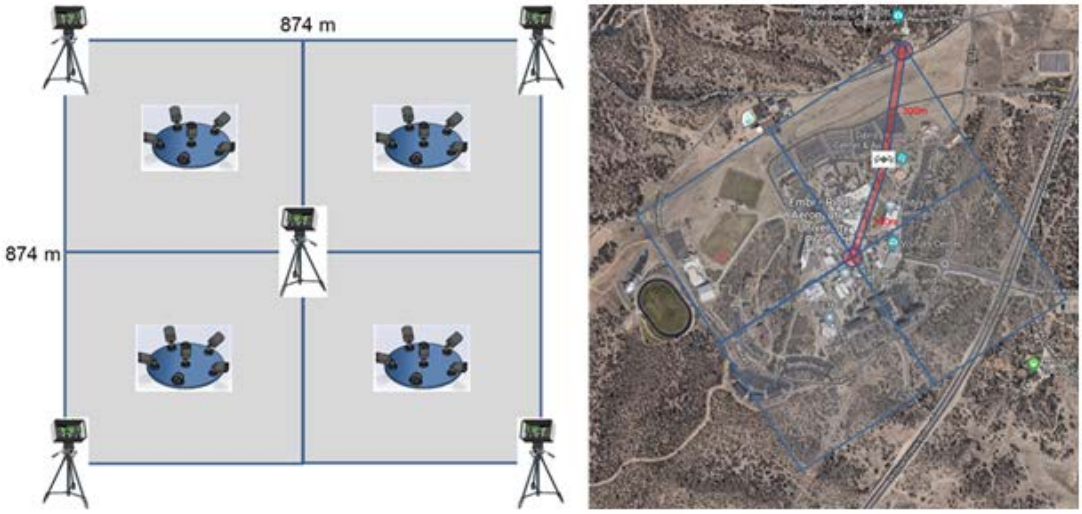

Figure 3. EO/IR and All-sky Camera Grid with ERAU Prescott Campus Coverage

The design is intended to be directly comparable to RADAR systems designed for sUAS with a similar 1 meter or smaller cross section with detection capability matrix in Table 1. The RADAR we are comparing to in the analysis is an X-band sufficient to track sUAS. The analysis shows that we are competitive, but we plan to further investigate with simulation and/or field testing with a NASA UTM partner in the future. The comparison in Table 1 and the working distance is based upon the two reference RADAR product specifications [14, 15].

While it is possible to also detect sUAS with a spectrum analyzer (another passive option), at this time we have chosen not to include this in our experimental configuration based on cost and the fact that it is most useful for radio-controlled drones compared to autonomous. There is of course some electromagnetic emission from an autonomous drone, but less so. If this shows promise, we could add spectrum analysis to our configuration in the future.

Table 1. Detection Capability Comparison Matrix for EO/IR + Acoustic and RADAR

Target Feature	EO / IR	Acoustic	Spectrum Analyzer	RADAR (dual polar)
Shape	X			X
Track	X	X		X
Texture, color	X			
Thermal	X			
Acoustic Spectrogram		X		
E-mag signature			X	
Range	< 1Km	< 100m	< 5Km	< 10Km

The acoustic detectors have yet to be prototyped and tested for feasibility, but have been characterized in preliminary work and will be placed with all-sky camera instruments shown in Figure 3. The fully compliant sUAS, is equipped with ADS-B, LIDAR for urban navigation and EO/IR for machine vision aided navigation, along with an HF (High Fidelity) IMU (Inertial Measurement Unit) with accelerometers, rate gyros and an electromagnetic compass [22]. The visual and acoustic detection and tracking can be verified in real-time with ADS-B and post flight with the HF IMU data using this fully compliant sUAS, which serves as an aerial Drone Net node.

Experiment Replication and Scaling

The Drone Net architecture is design to include a database with information sharing such that multiple locations can compare aerial object catalogs to improve machine learning supervised training for classification and identification. All of the Drone Net software, firmware and hardware is easily reproduced based on the reference architecture (and detailed design in progress) using off-the-shelf components, 3D printed parts for integration, and open source software [33]. Furthermore, all cameras and subsystems are portable to rural locations (EO/IR, all-sky cameras, acoustic arrays, compliant sUAS node, and ground station processing).

The cost of a 4 cell grid, as shown in Figure 3, is between $50K and as low as $30K, so it is quite feasible for use at regional airports, university campuses, business parks, and other typical urban and rural areas of interest that are within a 1 kilometer or smaller area like our Embry Riddle Prescott central campus or adjacent regional airport (PRC, Ernest A. Love Field). We have invited collaboration and are in discussions with other universities for collaborative testing and have joined the NASA UTM partner program.

We coordinate Part 107 compliant testing with our tower at PRC and have FAA registered Part 107 remote pilots who have waivers for VLOS (Visual Line of Sight) sUAS flights for our testing, but would like to work in the future with UPP locations (7 nationwide) to co-test with ground and aviation based RADAR with BVLOS rural and urban scenarios for UTM TCL-3 and TCL-4 test objectives in the future. It is quite feasible for us to pack up our instruments and field-deploy them at any site or install on roof-tops or pole-mounts for more permanent urban infrastructure testing.

Experiment Integration with UTM and ATC

The goal for the Drone Net experiments is to determine how feasible passive sensing is for UTM and as a method to notify ATC when non-compliant sUAS are operating in cells with general aviation and present a hazard requiring de-confliction. We are collaborating with ERAU Prescott ATC program researchers to provide notifications for issues of non-compliance within a 1-kilometer square cell so that an ATC FSS (Flight Support Specialist) could take appropriate action to ensure general aviation safety if an sUAS does not de-conflict as required by UTM (a rogue drone). Table 2 shows a classification of threat to general aviation by level of non-compliance.

Table 2. Severity of UTM Non-compliance and Threat to an ATC Cell

Compliance Description	Flight Plan	ADS-B	Compliance	ATC notification
Registered sUAS, registered remote pilot, flight plan filed, following flight plan, providing ADS-B, safe navigation aided by IMU, LIDAR, and machine vision.	X	X	Full	None
No ADS-B, unknown navigation equipment, standing waiver with Part 101 registered drone (e.g. hobby)	X		Full	None
Registered sUAS and remote pilot with ADS-B and safe navigation equipment, but not on filed flight plan.		X	Partial	Warning
No ADS-B, unknown navigation equipment, no standing waiver or filed flight plan, unknown registration (e.g. hobby drone possibly registered, but unknown)			Partial	Warning
No ADS-B, large visual size, no standing waiver or filed flight plan, not classified or identified as hobby drone, unexpected track, shape, texture, and color in visible and LWIR.			None	Safety Alert

DRONE NET EXPERIMENT SENSORS

The Drone Net system architecture includes multiple EO/IR nodes, multiple all-sky camera nodes, acoustic array nodes interfaced to all-sky cameras, and a more than fully compliant aerial node configured with ADS-B transceiver, EO/IR, LIDAR and an HF IMU. The block diagram of hardware elements, both ground and flight, is shown in Figure 4.

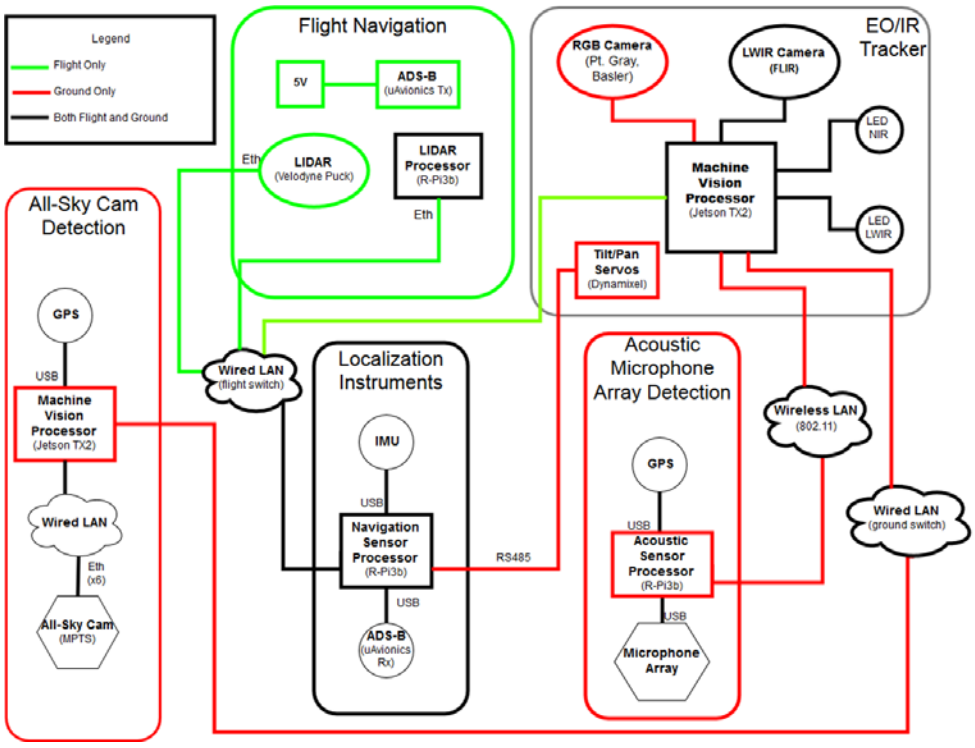

Figure 4. Block Diagram of all Drone Net Experiment Hardware Elements and Interfaces

All-Sky Camera

The all-sky camera should be the first instrument to detect an aerial object, based on motion alone, with the goal to simply determine an azimuth and elevation for an object of interest. The all-sky will send a wireless 802.11 message to the closest EO/IR narrow field tilt/pan tracker requesting classification and active tracking. The EO/IR will reply with affirmative and tracking started, or no-object of interest found. While an EO/IR node is tracking, the All-sky will not make further requests of that node until it is done tracking and no longer busy. If a new motion-based detection is made, it will send a notification to the next most near EO/IR node. If low-light operation is desired, NIR night-vision or even LWIR can be used, but LWIR has prohibitive resolution constraints.

The minimum resolution required is 2 megapixels per camera, but up to 20 megapixels per camera, such that the six-camera configuration is 12 to 120 megapixels, which can be processed by the MV processor node (e.g. NVIDIA Jetson TX2) to determine azimuth and elevation of potential sUAS (any moving object not filtered by erosion method to remove clouds, above statistical thresholds for noise, etc.). For initial prototyping and feasibility analysis of the all-sky camera construction, an off-the-shelf 1920x1080 resolution MPTS (MPEG Transport Stream) camera was used based on low-cost and ease of integration with gigabit Ethernet.

The need for finding intrinsic and extrinsic parameters of a camera is paramount to building a system based which would use the camera because these are known to have distortion because of various factors like image sensor, focal length, and the resolution. These parameters are constants and with a calibration and some remapping we can correct this. Furthermore, with calibration you may also determine the relation between the camera's natural units (pixels) and the real-world units (for example millimeters). For the distortion the OpenCV [7] software running on the all-sky camera image-processing system takes into account the radial and tangential factors.

For the distortion, image processing libraries such as OpenCV can be used to take into account the radial and tangential factors. For the radial factor a curve fit can be used such as:

$x_{distorted} = x(1+k_1r^2+k_2r^4+k_3r^6)$, $y_{distorted} = y(1+k_1r^2+k_2r^4+k_3r^6)$

So for an undistorted pixel point at (x,y) coordinates, its position on the distorted image will be ($x_{distorted}$, $y_{distorted}$). The presence of the radial distortion manifests in form of the "barrel" or "fish-eye" effect.

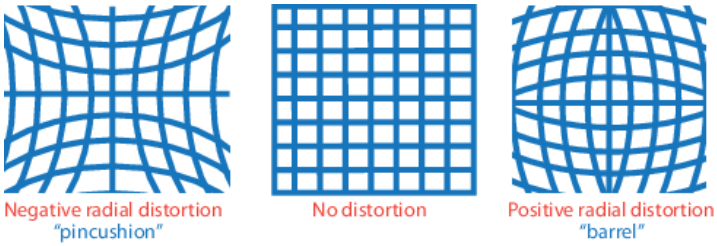

Figure 5. Distortion [6]

Tangential distortion occurs because the image taking lenses are not perfectly parallel to the imaging plane. It can be represented via the formulas:

$x_{distorted} = x + [2P_1xy+P_2(r^2+2x^2)]$, $y_{distorted} = y + [P_1(r^2 + 2y^2) + 2P_2xy]$

We have five distortion parameters which in OpenCV are presented as one row matrix with 5 columns as (K_1 K_2 P_1 P_2 K_3).

The intrinsic parameters include the focal length, the optical center, also known as the principal point, and the skew coefficient. The camera intrinsic matrix is defined as:

$$\begin{matrix} fx & 0 & cx \\ 0 & fy & cy \\ 0 & 0 & 1 \end{matrix}$$

The process of determining these two matrices is completed during the calibration process. Calculation of these parameters is done through basic geometrical equations. The equations used depend on the chosen calibrating objects. Currently OpenCV supports three types of objects for calibration: 1) classical black-white chessboard, 2) symmetrical circle pattern and 3) asymmetrical circle pattern. We used the classical black-white chessboard pattern for calibration. To calibrate each all-sky camera, images encapsulating this chessboard pattern must be provided in different orientations and at different distances. The goal is to determine the distortion matrix, camera matrix and use these to find the field of view of our camera [6] and [7].

Applying the camera intrinsic and extrinsic models to the array of six cameras, it is possible to minimize distortion and to correlate pixel locations from each camera to a specific elevation angle and azimuth. Figure 6 shows preliminary results of distortion correction.

Figure 6. Distortion Correction for Each All-sky Camera

Key optical parameters obtained from 10 images used in testing are:

1. Camera matrix: fx = 2471.81, fy = 2314.9, cx = 55.4883, cy = 0.202267
2. Distortion coefficients: K_1 = -0.11309 K_2 = -0.170633 P_1 = 10.0108727 P_2 = -0.00888144 K_3 = 0.151348
3. RMS re-projection error = 2.16958, Focal length = 6.93mm
4. Horizontal field of view = 40.158 degrees, Vertical field of view = 33.5669 degrees, Aspect ratio = 0.936518

Using 18 sample images provides refinement of the intrinsic parameters:

1. Camera matrix: fx = 1411.57, fy = 1421.72, cx = 719.732, cy = 518.797
2. Distortion coefficients: K_1 = -0.54306, K_2 = 0.331447 P_1 = 0.00118659 P_2 = 0.0387501 K_3 = -0.0360354
3. RMS re-projection error = 0.7266, Focal length = 3.96mm
4. Horizontal field of view = 70.27 degrees, Vertical field of view = 55.63 degrees, Aspect ratio = 1.0072

We can see that the camera extrinsic and intrinsic parameters depend on the number of input images provided. The RMS re-projection error is a good indicator of the accuracy of our obtained results. Ideally an accepted RMS re-projection error would be in the range of 0.1 to 1.0 and we can see that with 18 images we have obtained a RMS re-projection error of 0.7266 which would be an acceptable result.

Hence, we can construct our camera model with the field of views obtained (H_{fov}=70.27 degrees, V_{fov} = 55.63 degrees) and the diagonal field of view is ***sqrt***$((70.27)^2 + (55.63)^2)$ = 89.6246 degrees. Hence, we need at minimum four MPTS off-the-shelf cameras to obtain a 180-degree field of view for the all sky camera and a center camera (minimum of five). With the current reference design, the six-camera configuration with a pentagon configuration of cameras on a base and one center camera will oversample pixels with overlapping fields of view and/or use of cameras with slightly narrower field of view. For simplicity, square field of view would be ideal, but is generally hard to find, so an AR close to one such as 4:3 is preferable.

All-Sky Acoustic Detector

The all-sky acoustic detector shares goals and objectives with the all-sky camera, but can operate in low-lighting and bad weather beyond range of visible and NIR night-vision. As such, the all-sky acoustic can be used to supplement all-sky camera object of interest initial detection.

There are two setups about which we will discuss in this section. First, we have tested the feasibility of the "delay and sum" method for direction of arrival which is not quite accurate, but we have to use it for angle detection initially before calculating angles of arrival using MUSIC. In the second setup we have shown a MATLAB simulation of MUSIC algorithm and test results [35]. We are planning to integrate these two methods for a setup in which we can find direction of arrival of actual sound source where we will get coarse angle of arrival from the 8 MIC arrays on MATRIX creator shown in Figure 7, which is connected to the acoustic processor, with fine angle estimation provided using the MUSIC algorithm [13].

The first implementation tested is the "delay of sum". As we discussed in our first part of the goal we found a MATRIX creator board which has an 8-microphone array. Microphone arrays

have better performance than single wide aperture microphone even in the near field thus we are using arrays. The maximum ADC sampling rate our current prototype is 16 KHz and we are using an FPGA to run the delay of sum algorithm. At this point, we are characterizing the frequency band output for sUAS [22] and as such, while we have not yet performed experiment with sound signature coming from actual drone. First, direction of arrival estimation (DOA) determines the direction of the sound source whereas localization algorithms determine the distance to the sound source. The source is far-field and we can therefore consider the source as a point source. For initial feasibility testing we have assumed the source frequency of sound to be below 5 KHz to get accurate results based on restrictions we have because of microphone spacing.

In general, additional sensors yield more signal information and can help suppress noise and interference. The key to extracting information from the array is to exploit the fact that the signals arrive at the different sensors at different times due to the array geometry and signal angle. The direction of arrival (DOA) of a sound source is an important piece of information for any beamforming system. With this knowledge, the beam-forming can direct itself to capture signals coming only from the direction of arrival while ignoring others – by adding a delay stage to each of the array elements. The idea is simple; add a delay to each microphone such that the signals from a particular direction are aligned before they are summed. By controlling these arrays, the main lobe direction can be steered [34]. Based on the current configuration, because spacing of microphones is d = 4 cm, velocity of sound in air is assumed to be 340 m/s, and therefore the λ_{min} >= 2 * d, and maximum frequency is 4.25 KHz.

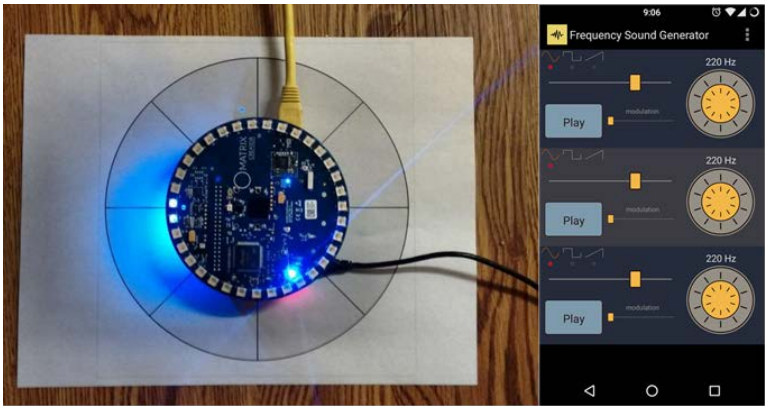

Figure 7. All-sky acoustic evaluation kit for beam-forming DOA

Frequencies of 1.5, 2.5 and 3.5 KHz were generated and the distance between the source and the microphone array were set to 5m and 10m. The detection accuracy is recorded in the Results section.

Table 3. Angle Estimation Compared to Actual in Feasibility Testing

5 meters from source				
Frequency [KHz]	1.5	2.5	3.5	Actual Angle
Detected angle	22.5	22.5	22.5	35
	67.5	67.5	67.5	70
	202.5	202.5	202.5	230
10 meters from source				
Frequency [KHz]	1.5	2.5	3.5	35
Detected angle	No detection	22.5	22.5	35
	No detection	67.5	67.5	70
	No detection	202.5	202.5	230

Range is limited with acoustic detection, so one concept for use is to place many of these beam-forming microphone arrays around the perimeter of an all-sky camera at a large radius to detect entry into the all-sky hemispherical field-of-view for sensor fusion (acoustic camera) and/or as a backup when the all-sky can't operate effectively due to weather or very low light (a more costly LWIR all-sky camera is another option to be explored).

The basic idea of MUSIC algorithm is to conduct characteristic decomposition for the covariance matrix of the received signal data, resulting in a signal subspace orthogonal with a noise subspace corresponding to the signal components. Then these two orthogonal subspaces are used to constitute a spectrum function, and by spectral peak search is used to detect DOA of signals.

To determine basic feasibility for the concept of refining coarse azimuth and elevation angle estimates from delay and sum using MUSIC as a second step, a MATLAB simulation was run for three signals (frequency bands = 1.5, 2.5, 3.5 KHz) at 35, 39, and 127 degrees azimuth with corresponding elevations of 63, 14, and 57 degrees. Figure 8 shows results for an 8-microphone array using Gaussian white noise sources.

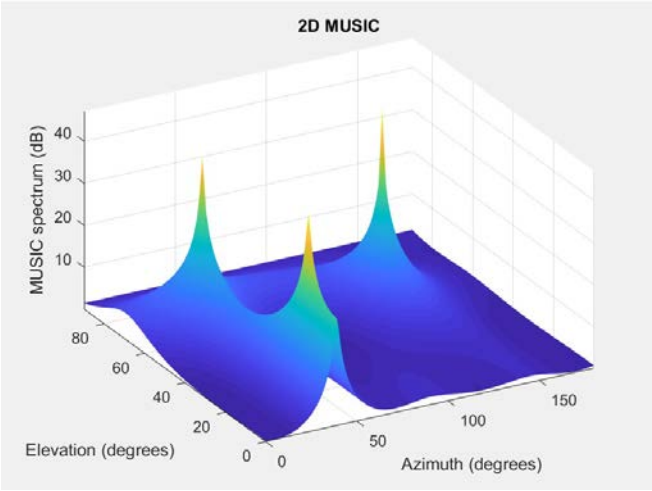

Figure 8. All-sky acoustic MUSIC refinement of Azimuth and Elevation estimation

The main challenge of acoustic azimuth and elevation estimation will be limited range of detection and issues with background noise. One fortuitous advantage of acoustic is that it can work better at night when background noise is lower and can simply be a backup or used to improve confidence in classification.

EO/IR Active Tracking and Classification

Tracking with accuracy and precision with the Drone Net architecture requires knowledge of each node location (provided by GPS), the point direction of the EO/IR nodes over time (tilt and pan) provided by a built-in IMU and localization of drones either via ADS-B, OEM navigation, or HF navigation for compliant drones. For non-compliant drones, the goal is to localize from EO/IR after coarse elevation and azimuth estimation provided by all-sky cameras and acoustic detectors using narrow field imaging.

More than Fully Compliant sUAS Node

The fully compliant sUAS is a Drone Net node used for validation and verification of our geometric truth model and human review so that we can have confidence in non-compliant detection and tracking data. For the purpose of supporting UAS Traffic Management (UTM) operation, in

the context of compliant drones, Automatic Dependent Surveillance-Broadcast (ADS-B) broadcasts (and reception) by the compliant drone(s) and reception by the Drone Net node(s) seems to offer a compelling localization solution. An ABS-B only solution does, however, present certain limitations.

The potential for congestion of ADS-B transmitters, given the proliferation of small private drones, can lead to "flooding" the RF spectrum and thereby rendering reception unreliable. The high-dynamic flight paths, which are feasible with a small UAS, may be underserved by the 2Hz update rate of the ADS-B location transmission and the latency of the data could be up to one second. The positional error of the WAAS GPS derived position reporting provided by ADS-B is in the 2-meter to 3-meter range.

In order to address some of the limitations of ADS-B based localization a high-fidelity (HF) navigation solution is being developed. Specifically, this approach employs a high-performance MEMS inertial measurement unit (IMU) (e.g., Sensonor STIM 300), which is better than tactical grade navigation sensors as seen in Figure 9, along with a multi-constellation GNSS receiver. This approach provides a greater than 100 Hz update rate with less than 1 millisecond latency and position reporting in the 1 meter, or better, range.

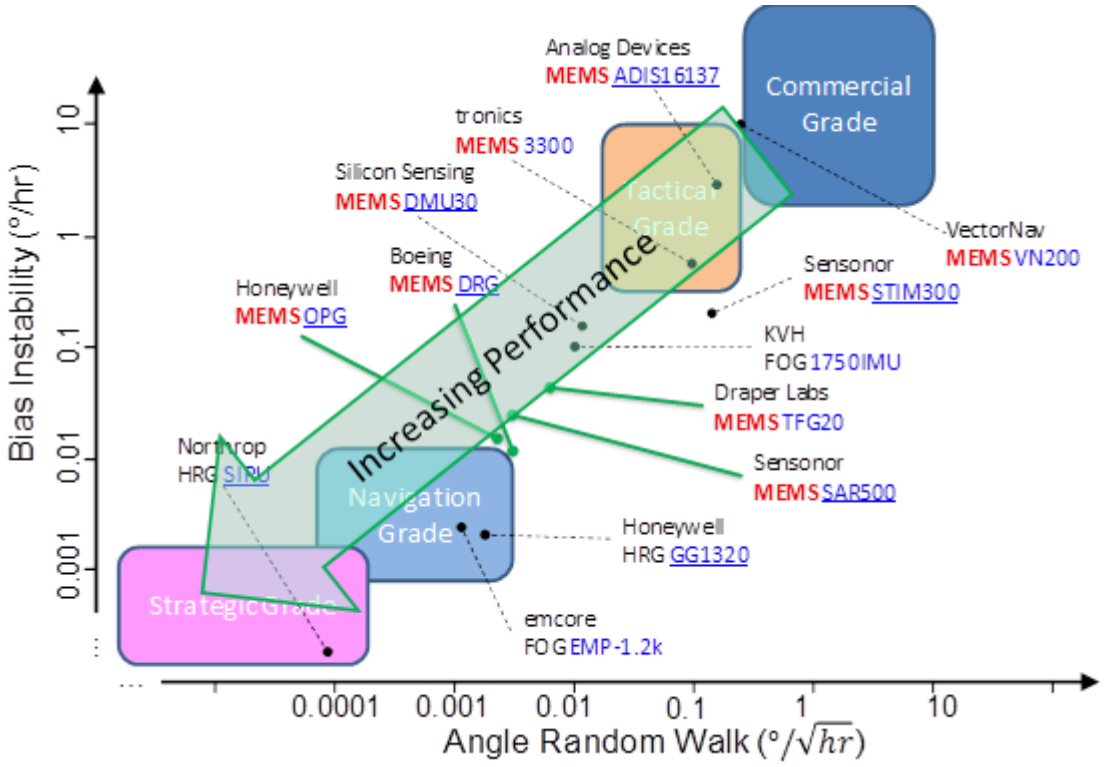

Figure 9. High Fidelity (HF) Navigation Performance

Our work with LIDAR and LWIR/visible cameras on our fully compliant sUAS has only recently been initiated, so we plan to characterize in the lab first and hope to fly with LIDAR + EO/IR in summer of 2018. The team has however started to work on LIDAR and LWIR fusion as shown in Figure 10.

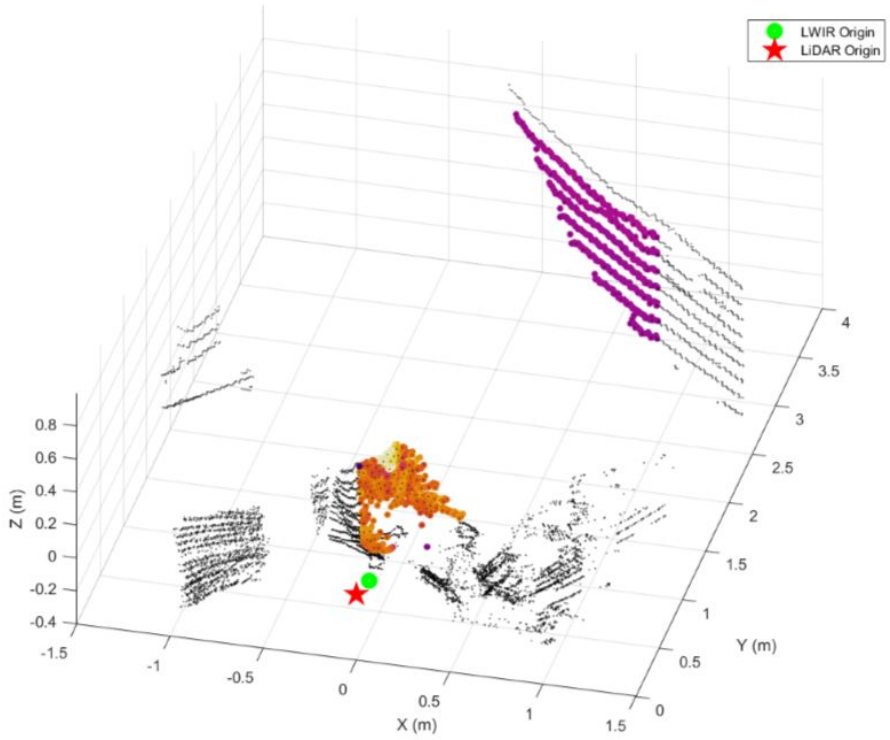

Figure 10. LIDAR Point Cloud from Lab Bench Test with LWIR image fusion

The fully compliant Drone Net flight node will thus be equipped with LIDAR as well as LWIR and visible imaging cameras for machine vision for urban navigation along with ADS-B tracking and ground EO/IR tracking. This is perhaps more than is needed for urban missions like parcel delivery, but our goal is to determine which navigational sensors, both active and passive on-board as well as on the ground, will allow for the most safe urban operation, allowing for BVLOS operation in environments that are outside of the scope of Part-107 today.

DRONE NET EXPERIMENT VERIFICATION

Verification of the fundamental architecture for Drone Net was completed in fall of 2017 with our second rural test. The results of this work were reported previously [22, 23]. While we have not yet fully determined the reliability, accuracy, precision and confidence in our localization of compliant and non-compliant sUAS, we have determined a test range configuration and limits, validated a semi-automated detection method, and manually verified observability and detection correlation of our results.

Trajectory Reconstruction Post Flight

I previous work in 2017, we showed that we are able to reconstruct a trajectory with reasonable track precision limited only by ADS-B and OEM navigation precision with our MATLAB re-simulation to provide field of view theoretical views compared to actual at the same point in time. More work needs to be done to determine overall reliability and the error in localization, but we have determined this is feasible.

Full Collection, Detection, Human Review Post Flight

Based on human review truth analysis in prior work [23], we know we can use human review for design validation and verification, but also for deployed operations to enhance MV/ML super-

vised learning methods based on new work done with the human reviewed images we tested with CNN (Convolutional Neural Networks) for this paper. The long-term goal is to make MV/ML software development and evolutionary improvement process whereby algorithms can be tested and compared off-line with the aerial catalog image database, but also in real-time when deployed to embedded EO/IR nodes. The all-sky cameras are envisioned to only need "lizard brain" intelligence where they simple detect using salient object motion detection with more intelligent classification provided by the EO/IR, further refinement provided by the aerial catalog MV/ML and the final analysis provided by human review and re-simulation.

DRONE NET AUTOMATION EXPERIMENT

The overall long-term goal for Drone Net is software design and development for this sensor network with cloud based MV/ML to further analyze real-time data from camera embedded processors to catalog tracking episodes (detection, classification, and potential identification from first detection until loss of tracking). The tracking in real-time will issue of alerts to subscribing ATC locations as well as logging for web browsing of sUAS traffic for forensic purposes.

Messaging Protocol between Drone Net Elements

The Drone Net software detailed design is still in progress, but conceptually messages and event notifications will have to be sent between each node, starting with the all-sky camera and/or all-sky acoustic detectors which can either broadcast or select the closest EO/IR camera node for tilt/pan narrow field re-detection and tracking. Once an EO/IR is actively tracking, it will be busy, and any new all-sky detections can either be directed to an idle redundant EO/IR camera along a diagonal for the same grid cell, or simply ignored (this needs further analysis in simulation or with larger networks). Based upon EO/IR tracking and eventual classification and potential identification based on consultation with the aerial object catalog, the EO/IR node that is tracking will transfer tracking files to the aerial catalog and cloud based MV/ML server per Drone Net installation.

The aerial catalog can further analyze a more complete track to determine which notification state an aerial object warrants from Table 2 (none, warning, or alert) to be issued to ATC if an ATC FSS location subscribes to this service. If not ATC FSS location is subscribing to Drone Net installation services, the condition would simply be logged with the tracking data for this episode of events (an episode will include all data from initial detection until loss of tracking). Re-detection is possible, but most likely Drone Net won't attempt to link or concatenate episodes. Along with real-time notification, it is envisioned that web services can provide browsing for forensic analysis of sUAS traffic for security and safety issues that do not need to be solved in real-time.

Full Collection, Detection, Machine Learning Post Flight

The goal of the off-line training and validation for MV/ML for Drone Net is to use the large data sets captured over time, such as the images in Figure 11, by the Drone Net project in the always growing aerial catalog and apply different methods for object detection leveraging currently used machine learning methods for comparison of performance between competing machine learning methods ranging from CNNs (Convolutional Neural Networks) to SVM (Support Vector Machines) to Bayesian methods such as DBN (Deep Belief Networks) using images collected from "the wild" where simple detection and salient object detection algorithms are used to capture many images continuously based on simple triggers like motion, shape, track characteristics, and from compliant test sUAS such as the Drone Net aerial node equipped with ADS-B (known to be in the field of view and known identity by registration). Primarily, two different object detection methods were implemented: Faster RCNN using Tensorflow and Single Shot Detection using Tensorflow. Faster RCNN uses region proposals to classify object proposals using deep convolu-

tional networks. Single shot detection uses different activation maps for prediction of classes and bounding boxes.

Figure 11. Example Drone Net Images from Motion Detection (LWIR)

Faster RCNN [10], the first algorithm used to implement object detection is built on the Tensor-Flow platform. Before we talk about Faster R-CNN, let's understand their predecessors: R-CNN and Fast R-RCNN. R-CNN [8] creates region proposals using a process called Selective Search which looks at the image through windows and tries to group together pixels by texture, color, or intensity. Once these proposals are created, R-CNN warps this region to a square, and passes it through to a CNN. The final layer of this CNN is a Support Vector Machine that identifies the object. But these passes are computationally tedious and are about 2000 passes per image.

In Fast R-CNN [9], the CNN is first run once per image, and then share this computation across the 2000 proposals. This is called Region of Interest Pooling. The features for each region are obtained by selecting a corresponding region from the CNN's feature map, and pooled together. This decreases the feature passing from 2000 per image to 1 per image. Another improvement is that Fast R-CNN uses a single network to compute feature extraction (CNN), identification (SVM) and bounding boxes (regression).

Further computation was decreased in Faster R-CNN, developed in 2015. Faster R-CNN uses CNN for feature extraction and identification, so we only need to train the CNN in this algorithm.

The results of R-CNN testing with motion detect triggered images showed stable precision of 80% as shown in Figure 12 for a mixture of visible and LWIR images of all objects interest initially classified as drones based on previous work [23].

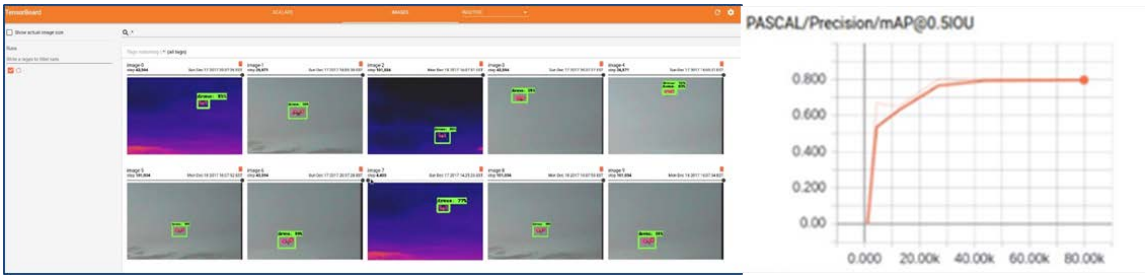

Figure 12. Results from R-CNN MV/ML Classification with Drone Net Detection Images

The second algorithm implemented as part of this independent study was Single Shot Detection [11]. The SSD approach is a feed-forward convolutional network with multiple layers that provide a finer accuracy on objects with different scales. This will output a fixed-size set of bounding boxes and confidence scores for detection. This is followed by a non-maximum suppression step to produce the final detection, where the bounding boxes with the most overlap score are selected. For Single Shot Detection, the evaluation was run 15,608 steps. As a result, the performance shoots from 0 to 0.95 in the single step as shown in Figure 13.

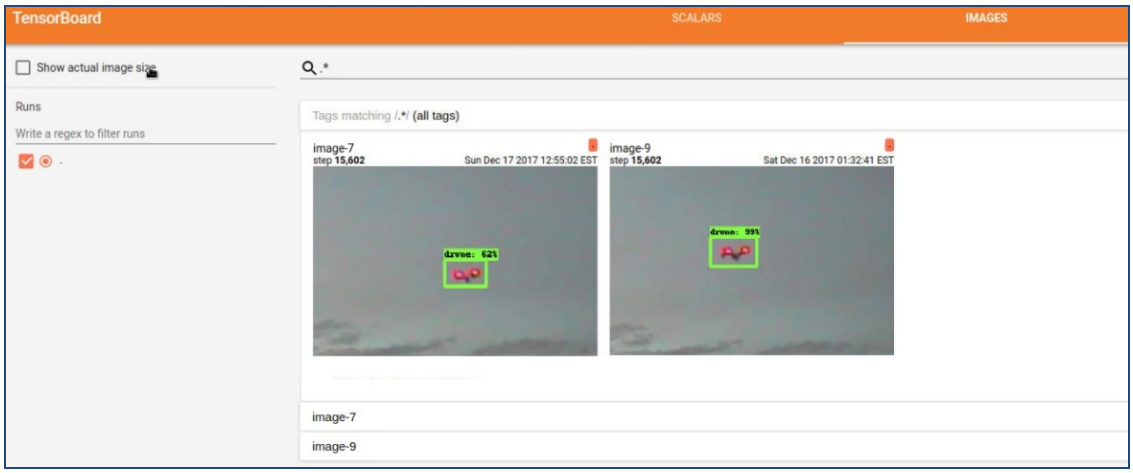

Figure 13: Evaluation by detecting test images: SSD model

Trained CNNs using the Drone Net aerial catalog will be used to deploy a pre-trained CNN for on-line real-time classification on a GP-GPU such as the NVIDIA *Tegra X2*. More work is needed to determine the best MV/ML algorithms for Drone Net classification of "drone", "aircraft", "rotorcraft", "bird", "bug", etc. rejection objects not of interest as shown in Figure 14. Most likely only three classifications are necessary – "drone", "general aviation", "other", but it might help to train for specific aerial objects – something that remains to be determined. As was found in earlier work, normal operation of the motion detect salient object detection layer results in many objects that are not of interest to UTM, where our system has a high false positive rate based on bugs, bird, bats, etc. [23].

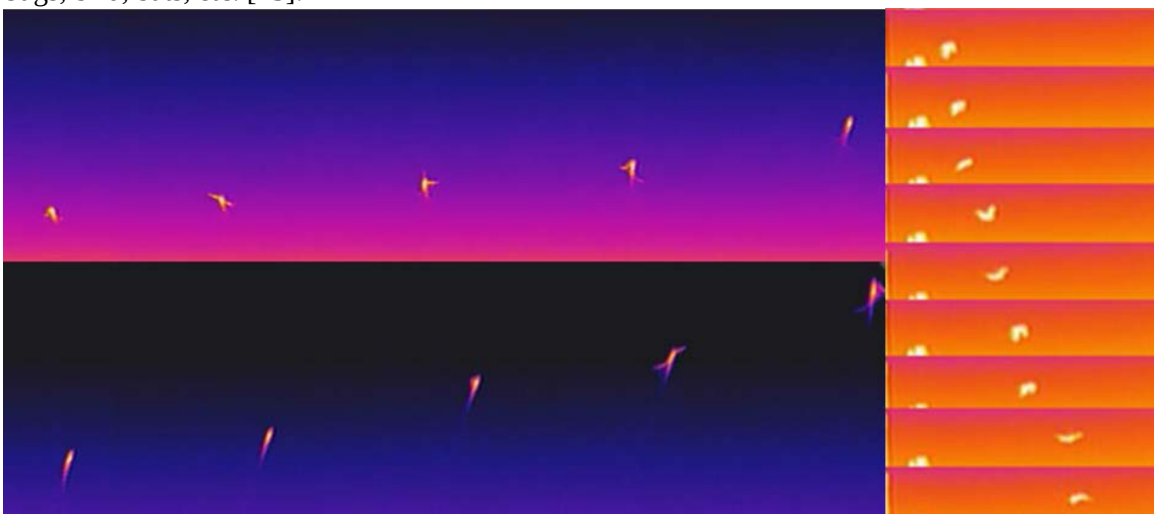

Figure 14: Aerial Objects Not of Interest to UTM that must be ignored [23]

Aerial Catalog Concepts

The Drone Net aerial catalog is critical to the long-term success of our strategy, whereby the depth and variety of confirmed classifications and identifications verified by human review is hypothesized to lead to evolutionary precision improvement over time and as the number of Drone Net installations and cameras are scaled. Evidence that this is true is based on prior related work for large scale MV/ML projects [12]. One concept we are exploring is to use gamification for the human review and another is a credit system, perhaps using a Drone Net blockchain cur-

rency to pay for detection and tracking data by first building up credit with time spent providing classifier human review verification. To date, human review has been done with a semi-automated tool called Auto-it. For compliant nodes, the plan is to make use of ADS-B and HF navigation data with re-simulation to mark all drone images based on geometric visibility assertion (which can also be compared to human review). In general, the aerial catalog quality for classifications can be statistically measured in terms of human review reliability and confidence as well as geometric (two truth models).

DRONE NET FIELD TESTING RESULTS

To date, two rural tests north of ERAU Prescott in uncontrolled class-G airspace with VLOS drone flights (two at a time, one acting in a compliant fashion with ADS-B continuous transmission and one without) have been completed. Likewise, two urban tests on campus in class-D controlled airspace based on Part-107 tower waivers with Ernest Love field for flights by a Part-107 certified remote pilot. For the urban tests, we completed the same two drone, one compliant, one not compliant testing on February 25, 2018 [31] and one with a simple lift-off test of our larger ALTA6 drone to determine limits of VLOS with unaided viewing by the remote pilot (walking underneath) and by an observer and cameras at the far end of the diagonal shown in Figures 2 and 3 [32]. The first urban test essentially repeated our last rural test and focused on localization of the compliant drone using the built-in OEM (Original Equipment Manufacturer) navigation and ADS-B data to check presence in our camera field of view compared to predicted observability with our MATLAB analysis tools [22]. The second urban test focused on validation of our grid cell design to cover our campus as shown in Figures 2 and 3 along with verification of visible and LWIR camera pixel extents at the working distance of 617.5 meters. Future tests planned include a more complete configuration with semi-permanent EO/IR and all-sky installations with one compliant and one non-compliant drone and VLOS testing within the test cell, followed by expansion to the four-cell grid.

Prior Rural Testing Feasibility Summary

The prior rural testing completed used a single EO/IR camera and VLOS drone operations in uncontrolled class-G airspace with adherence to Part-107 rules. The main objective of these tests were validation of our two methods of truth analysis for detection and classification: 1) geometric truth based on ADS-B and OEM navigation data and correlation of detection images with re-simulation of observability based on EO/IR location and pointing along with compliant drone localization; 2) human review of detection images for agreement that they contain the drone of interest. More work is needed to automate the production of ROC, PR (Precision Recall) and F-measure curves, but ROC analysis has been done manually in prior work. Combined with MV/ML we anticipate ability to detect with accuracy similar to RADAR or better and to classify and identify objects of interest (which may not be possible with RADAR alone). More testing, analysis, and direct comparison to RADAR are however needed in future UTM testing, so at this point, we have determined feasibility, but not yet comparative performance.

Recent Urban Feasibility Testing Summary

At the time of the writing of this paper, we have completed data collection for both urban testing scenarios and visual feasibility of our test grid and cell design, but we are still working on fully analyzing our localization, observability and ROC performance. It is likely that we will need to re-test as we encountered logistical challenges including high winds in our 3/25/2018 testing (up

to 20 MPH or more) and based upon limitations of flight restrictions to adhere to Part-107 and campus safety rules during the school year.

CONCLUSION

The Drone Net architectural reference is complete and openly available for replication and re-use including hardware, firmware and software. The goal is to collaborate with interested universities and industry in future UTM tests at UPP (UTM Partner Program) test sites that have waivers for BVLOS operation and complimentary resources such as ground RADAR with characteristics suitable for sUAS detection and tracking. To date, four experiments have been completed including two rural [22] and two urban VLOS feasibility tests with results provided in this paper. We would like to invite potential industry and other academic collaborators to work with us on urban UTM through NASA UPP, FAA IPP, or other programs for field testing of sUAS operations and systems support for national airspace integration. At this point, we believe we have an "open" system architecture and experimental plan which can help both industry and government agencies with performance evaluation and comparison of passive and active sensing methods for UTM.

ACKNOWLEDGMENTS

We would like to acknowledge testing support provided by the Embry Riddle Aeronautical University UAS program and their pilots as well as alumni pilot Ricardo Fernandez. This research has been supported by an internal ARI (Accelerate Research Initiative) grant from Embry Riddle. The project has also been supported by the ICARUS group (https://pluto.pr.erau.edu/~icarus/) faculty and associated graduate and undergraduate students as well as the CU Boulder ESE (Embedded Systems Engineering) program graduate students who have participated in independent research on Drone Net.

REFERENCES

[1] Kopardekar, Parimal, et al. "Unmanned aircraft system traffic management (utm) concept of operations." *AIAA Aviation Forum*. 2016.

[2] Mohajerin, Nima, et al. "Feature extraction and radar track classification for detecting UAVs in civillian airspace." *Radar Conference, 2014 IEEE*. IEEE, 2014.

[3] Aker, Cemal, and Sinan Kalkan. "Using Deep Networks for Drone Detection." *arXiv preprint arXiv:1706.05726* (2017).

[4] Abadi, Martín, et al. "Tensorflow: Large-scale machine learning on heterogeneous distributed systems." *arXiv preprint arXiv:1603.04467* (2016).

[5] Deng, Jia, et al. "Imagenet: A large-scale hierarchical image database." *Computer Vision and Pattern Recognition, 2009. CVPR 2009. IEEE Conference on*. IEEE, 2009.

[6] Mathworks, https://www.mathworks.com/help/vision/ug/camera-calibration.html#bu0niww.

[7] OpenCV, https://docs.opencv.org/trunk/d4/d94/tutorial_camera_calibration.html.

[8] *Rich feature hierarchies for accurate object detection and semantic segmentation* by Ross Girshick, Jeff Donahue, Trevor Darrell, Jitendra Malik

[9] *Fast R-CNN* by Ross Girshick

[10] *Faster R-CNN: Towards Real-Time Object Detection with Region Proposal Networks* by Shaoqing Ren, Kaiming He, Ross Girshick, and Jian Sun

[11] *SSD: Single Shot MultiBox Detector* by Wei Liu, Dragomir Anguelov, Dumitru Erhan, Christian Szegedy, Scott Reed, Cheng-Yang Fu1, Alexander C. Berg

[12] Karpathy, Andrej, and Li Fei-Fei. "Deep visual-semantic alignments for generating image descriptions." *Proceedings of the IEEE conference on computer vision and pattern recognition*. 2015.

[13] Gupta, Pooja, and S. P. Kar. "MUSIC and Improved MUSIC algorithm to Estimate Direction of Arrival." *Communications and Signal Processing (ICCSP), 2015 International Conference on*. IEEE, 2015.

[14] EECRanger X5 RADAR specification - http://www.eecweathertech.com/pdf/EEC-Ranger-Specs.pdf.

[15] Echodyne MESA-DAA RADAR specification - https://echodyne.com/wp-content/uploads/2017/05/MESA-DAA-Product-Sheet.pdf.

[16] February 25, 2018 urban testing results - https://pluto.pr.erau.edu/~icarus/AUVSI-2018/UTM-Urban-2-25-18/

[17] March 25, 2018 urban testing results for VLOS limits - https://pluto.pr.erau.edu/~icarus/AUVSI-2018/UTM-Urban-3-25-18/

[18] S. Siewert, Andalibi, S. Bruder, I. Gentilini, J. Buchholz, "*UAS Integration, Application, Education and Innovation - Drone Net Architecture for UAS Traffic Management Status*", ERAU President's Council on UAS National Airspace Integration and Applications, Daytona Beach, Florida, November 30, 2017.

[19] S. Siewert, Andalibi, S. Bruder, I. Gentilini, J. Buchholz, "*Drone Net – Big Data, Machine Vision and Learning Challenge and Opportunity*", invited speaker, 5th Annual Global Big Data Conference, Silicon Valley, August 29-31, 2017.

[20] S. Siewert, Andalibi, S. Bruder, I. Gentilini, J. Buchholz, "*Drone Net: Using Tegra for Multi-Spectral Detection and Tracking in Shared Air Space*", GPU Technology Conference, Silicon Valley, May 8-11, 2017.

[21] S. Siewert, "*The Computational Photometer – Hybrid FPGA Digital Video Transformation for 3D*", IEEE Alaska Section Technical Presentation, Anchorage, Alaska, January 28, 2014.

[22] S. Siewert, M. Andalibi, S. Bruder, I. Gentilini, J. Buchholz, "Drone Net Architecture for UAS Traffic Management Multi-modal Sensor Networking Experiments", IEEE Aerospace Conference, Big Sky, Montana, March 2018.

[23] S. Siewert, M. Vis, R. Claus, R. Krishnamurthy, S. B. Singh, A. K. Singh, S. Gunasekaran, "*Image and Information Fusion Experiments with a Software-Defined Multi-Spectral Imaging System for Aviation and Marine Sensor Networks*", AIAA SciTech 2017, Grapevine, Texas, January 2017.

[24] S. Siewert, V. Angoth, R. Krishnamurthy, K. Mani, K. Mock, S. B. Singh, S. Srivistava, C. Wagner, R. Claus, M. Vis, "*Software Defined Multi-Spectral Imaging for Arctic Sensor Networks*", SPIE Proceedings, Volume 9840, Algorithms and Technologies for Multispectral, Hyperspectral, and Ultraspectral Imagery XXII, Baltimore, Maryland, April 2016.

[25] S. Siewert, J. Shihadeh, Randall Myers, Jay Khandhar, Vitaly Ivanov, "*Low Cost, High Performance and Efficiency Computational Photometer Design*", SPIE Proceedings, Volume 9121, Sensing Technology and Applications, Baltimore, Maryland, May 2014.

[26] S. Siewert, M. Ahmad, K. Yao, "*Verification of Video Frame Latency Telemetry for UAV Systems Using a Secondary Optical Method*", AIAA SciTech 2014, National Harbor, Maryland, January 2014.

[27] Black Sage, https://www.blacksagetech.com/

[28] Drone Shield, https://www.droneshield.com/

[29] Dedrone, http://www.dedrone.com/en/

[30] SRC Gryphon, https://www.srcgryphonsensors.com/

[31] Drone Net, test results, February 25, 2018, https://pluto.pr.erau.edu/~icarus/AUVSI-2018/UTM-Urban-2-25-18/

[32] Drone Net, test results, March 25, 2018, https://pluto.pr.erau.edu/~icarus/AUVSI-2018/UTM-Urban-3-25-18/

[33] Drone Net, open source software, https://github.com/dronenet

[34] http://www.labbookpages.co.uk/audio/beamforming/delaySum.html

[35] https://www.edaboard.com/showthread.php?79938-MUSIC-Algorithm-for-Direction-Finding